

# Terahertz inversionless lasing from a cavity-embedded two-dimensional electron gas in asymmetric quantum wells

Simone De Liberato<sup>1</sup>, Cristiano Ciuti<sup>1</sup>, and Chris C. Phillips<sup>2</sup>

<sup>1</sup> *Laboratoire Matériaux et Phénomènes Quantiques,*

*Université Paris Diderot-Paris 7 and CNRS, UMR 7162, 75013 Paris, France and*

<sup>2</sup> *Physics Department, Imperial College London, London SW7 2AZ, United Kingdom*

Electric dipole transitions between different cavity polariton branches or between dressed atomic states with the same excitation number are strictly forbidden in centro-symmetric systems. For doped quantum wells in semiconductor microcavities, the strong coupling between an intersubband transition in the conduction band and a cavity mode produces two branches of intersubband cavity polaritons, whose normal-mode energy splitting is tunable and can be in the terahertz region. Here, we show that, by using asymmetric quantum wells, it is possible to have allowed dipolar transitions between different polaritonic branches, leading to the emission of terahertz photons. We present a quantum field theory for such a system and predict that high-efficiency, widely tunable terahertz lasing can be obtained.

The resonant coupling between a photon mode and an electronic transition can produce hybrid light-matter eigenstates, such as the well-known dressed states in atomic cavity quantum electrodynamics [1] or the polariton excitations in solid-state systems [2]. In general, if one considers a doublet of dressed states, the electric dipole transition between these two states is strictly forbidden in any centro-symmetric system. Analogously, in the case of cavity polaritons, a transition from the upper to the lower polariton branch cannot be accompanied by any photon emission and can be only of non-radiative origin (e.g., via phonon emission [3]). Recently though, it has been shown that, in exciton-polariton systems, the application of an electric field produces hybridisation of internal motion exciton states with different parity, thus breaking such a selection rule [4–6]. This enables transitions between different exciton-polariton states and in principle paves the way to integrated terahertz (THz) sources where the excitation is provided by a near-infrared pump with potentially significant quantum efficiencies (up to 1.5%).

Indeed, sources emitting in the THz region of the electromagnetic spectrum are a subject of intense investigations both for fundamental physics and applications. In fact the THz region represents a technological gap that can be covered only with difficulty, either with electronic devices (at lower frequencies), or with lasers (at higher frequencies). A great research effort has been accomplished to extend semiconductor quantum cascade lasers [7] to the THz region [8]: in such devices transitions occurs from quantized subbands in the conduction band of suitably designed multiple quantum well structures. Although THz quantum cascade lasers are developing [9], fundamental limitations occur because the radiative lifetimes of the excited electronic states are long compared to the intrinsic fast non-radiative recombination channels that arise from efficient electron-phonon scattering (at least in the case of incoherent electronic excitations [10]).

In the case of intersubband transitions, it is possible to reach the strong light-matter coupling regime by embedding a structure containing multiple doped quantum wells in microcavity resonators [11–14], leading to the creation of so-called intersubband cavity polariton modes. In such a system, it is possible to control in-situ the value of the polariton splitting [15–17] and it is possible to engineer the intersubband transitions in a very flexible way [18]. A fundamental unexplored question is whether in such a class of intersubband systems it would be possible to have efficient radiative transitions between polariton branches.

In this letter, we show that breaking the wavefunction symmetry using asymmetric quantum wells enables radiative transitions between different intersubband polariton branches, leading to intrinsically efficient, widely tunable THz lasing without electronic population inversion. We develop a quantum theory describing such process and determine the overall efficiency of the THz emission, in a way that takes into account the nonbosonicity of intersubband excitations [3, 19]. We have calculated, both analytically and numerically, the intrinsic quantum efficiency for the considered process showing that, for realistic parameters, unprecedented quantum efficiencies are achievable.

Let us start by considering a quantum Hamiltonian describing two parallel semiconductor conduction subbands coupled to a quasi-resonant microcavity photon mode, in the rotating wave approximation (RWA), namely

$$H = \sum_{\mu \in \{1,2\}, \mathbf{k}} \hbar \omega_{\mu}(\mathbf{k}) c_{\mu, \mathbf{k}}^{\dagger} c_{\mu, \mathbf{k}} + \sum_{\mathbf{q}} \hbar \omega_{\text{ph}}(\mathbf{q}) a_{\mathbf{q}}^{\dagger} a_{\mathbf{q}} \quad (1) \\ + \sum_{\mathbf{k}, \mathbf{q}} \hbar \chi(\mathbf{q}) a_{\mathbf{q}}^{\dagger} c_{1, \mathbf{k}}^{\dagger} c_{2, \mathbf{k}+\mathbf{q}} + \hbar \chi(\mathbf{q}) a_{\mathbf{q}} c_{2, \mathbf{k}+\mathbf{q}}^{\dagger} c_{1, \mathbf{k}},$$

where  $c_{\mu, \mathbf{k}}^{\dagger}$  and  $a_{\mathbf{q}}^{\dagger}$  are, respectively, the creation operators for an electron in the quantum well conduction subband  $\mu$  with in-plane wave vector  $\mathbf{k}$  and a microcavity photon with in-plane wave vector  $\mathbf{q}$ . Their re-

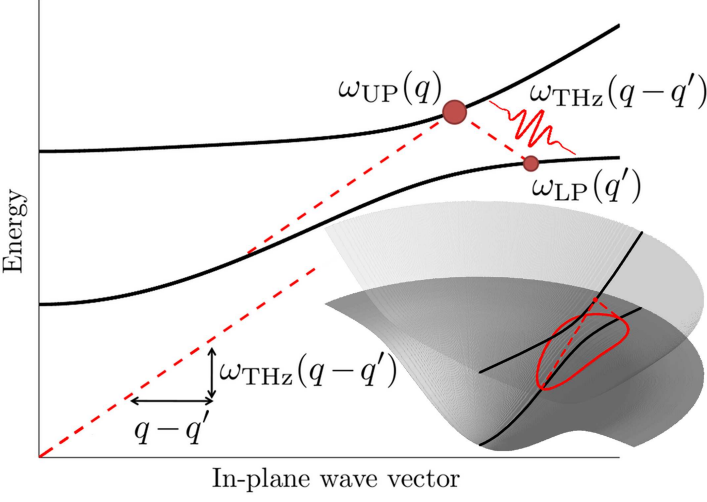


FIG. 1: Typical energy dispersion of the lower and upper intersubband cavity polariton branches (black solid lines), and of the THz mode of the metallic cavity (red dashed lines). All the allowed final states for the radiative process under examination, in which an upper polariton scatters into a lower polariton plus a THz photon, are marked in red on the 3D image. For clarity the lightcone of the THz mode is also shown originating from the upper polariton mode. The process highlighted by red dots corresponds to the forward scattering process considered in the text, such that  $\mathbf{q}$  and  $\mathbf{q}'$  are parallel.

spective energies are  $\hbar\omega_\mu(k)$  and  $\hbar\omega_{\text{ph}}(q)$ , with  $\hbar\omega_2(k) = \hbar\omega_1(k) + \hbar\omega_{12}$ . The coefficient  $\hbar\chi(q)$  quantifies the light-matter coupling and it is proportional to the intersubband dipole  $z_{12} = \int dz z \psi_1(z) \bar{\psi}_2(z)$ , where  $\psi_\mu$  is the wave function along  $z$ , normal to the quantum well plane, of an electron in subband  $\mu$ . If we consider an intersubband energy  $\hbar\omega_{12}$  in the mid-infrared region, the Coulomb interaction [13, 20, 21] can be neglected to a first approximation. All the interactions are spin conserving and are between states in the same quantum well, so for simplicity we omit the spin and quantum well indices. Due to the intersubband transition selection rules, only the Transverse Magnetic (TM) cavity mode couples to electrons. Introducing the (approximately bosonic) bright intersubband operator  $b_{\mathbf{q}}^\dagger$  [12],

$$b_{\mathbf{q}}^\dagger = \frac{1}{\sqrt{N}} \sum_{\mathbf{k}} c_{2,\mathbf{k}+\mathbf{q}}^\dagger c_{1,\mathbf{k}}, \quad (2)$$

the intersubband dynamics from Eq. (1) can be modeled by the effective Hamiltonian

$$\begin{aligned} H' &= \hbar \sum_{\mathbf{q}} \omega_{\text{ph}}(q) a_{\mathbf{q}}^\dagger a_{\mathbf{q}} + \omega_{12} b_{\mathbf{q}}^\dagger b_{\mathbf{q}} + \Omega(q) (a_{\mathbf{q}}^\dagger b_{\mathbf{q}} + b_{\mathbf{q}}^\dagger a_{\mathbf{q}}), \\ &= \sum_{j \in \{\text{LP}, \text{UP}\}, \mathbf{q}} \hbar\omega_j(q) p_{j,\mathbf{q}}^\dagger p_{j,\mathbf{q}}, \end{aligned} \quad (3)$$

where  $N = n_{\text{QW}} N_{2\text{DEG}} S$  is the total number of electrons

in the structure ( $n_{\text{QW}}$  is the number of quantum wells,  $N_{2\text{DEG}}$  is the density of the two-dimensional electron gas and  $S$  is the transverse surface) and  $\Omega(q) = \sqrt{N}\chi(q)$  is the vacuum Rabi frequency. The Hamiltonian in Eq. (3) can be diagonalized in terms of the normal-mode polariton operators  $p_{j,\mathbf{q}}^\dagger = x_{j,\mathbf{q}} a_{\mathbf{q}}^\dagger + y_{j,\mathbf{q}} b_{\mathbf{q}}^\dagger$ , where  $x_{j,\mathbf{q}}$  and  $y_{j,\mathbf{q}}$  are the (real) Hopfield coefficients that denote the light and matter fractions of the polaritonic excitations respectively. In Fig. 1, a sketch of the typical energy-momentum dispersion for the lower and upper polariton branches is shown.

For intersubband cavity polaritons with energies in the mid-infrared, transitions between the upper and lower polariton branch are typically in the THz region of the spectrum. The cavity also contains photon modes at these THz frequencies, and here we consider the process, depicted in Fig. 1, where a polariton is first excited into the upper branch with a pump beam, and then scatters to the lower branch by emitting a THz photon into the cavity. Such a coupling to the low energy THz modes is described by the interaction term:

$$H_{\text{int}} = e\hat{\mathbf{r}} \sum_{\mathbf{q}} \sqrt{\frac{\hbar\omega_{\text{THz}}(q)}{2\epsilon_0\epsilon_r S L_{\text{cav}}}} (\alpha_{\mathbf{q}} e^{i\hat{\mathbf{r}}\mathbf{q}} + \alpha_{\mathbf{q}} e^{-i\hat{\mathbf{r}}\mathbf{q}}), \quad (4)$$

where  $L_{\text{cav}}$  is the microcavity thickness,  $\hat{\mathbf{r}}$  the electron position operator and  $\alpha_{\mathbf{q}}^\dagger$  is the creation operator of the low energy THz cavity photon with energy  $\hbar\omega_{\text{THz}}(q)$ . For definiteness, in this letter we will consider the case of a metallic cavity, in which  $\alpha_{\mathbf{q}}$  is the TEM mode with linear dispersion [14], while  $a_{\mathbf{q}}$  belongs to an excited cavity branch, but other configurations are possible.

The matrix element describing the process illustrated in Fig. 1, in which a polariton jumps from the upper to the lower branch by emitting a THz photon, reads

$$\begin{aligned} \langle G | \alpha_{\mathbf{p}} p_{\text{LP},\mathbf{q}'} H_{\text{int}} p_{\text{UP},\mathbf{q}}^\dagger | G \rangle &= y_{\text{UP},\mathbf{q}} y_{\text{LP},\mathbf{q}'} e^{\Delta z} \sqrt{\frac{\hbar\omega_{\text{THz}}(p)}{2\epsilon_0\epsilon_r S L_{\text{cav}}}} \\ &\times \delta(\mathbf{q} - \mathbf{q}' - \mathbf{p}), \end{aligned} \quad (5)$$

where  $|G\rangle = \prod_{k < k_F} c_{1,\mathbf{k}}^\dagger |0\rangle$  is the Fermi ground state of the electronic system,  $|0\rangle$  is the vacuum state and  $\Delta z = \int dz z [|\psi_2(z)|^2 - |\psi_1(z)|^2]$  is the interbranch dipole, representing the distance between the mean electron positions in the two electronic subbands. As we have anticipated, this scattering process occurs only in asymmetric systems, where  $\Delta z \neq 0$ .

It is apparent from Fig. 1 that, for a given initial upper polariton mode, there is a continuum of final modes conserving both energy and momentum, given by the intersection between the lightcone of the THz mode irradiating from the initial upper polariton mode and the lower polariton branch. From Eq. (5) we see that the final mode with the larger value of  $q'$ , that is the one with the highest matter fraction  $y_{\text{LP},\mathbf{q}'}$ , is generally the

one most likely to win in a mode selection competition in a THz cavity. For definiteness then, in the following, we will confine our attention to just the forward scattering process shown in Fig. 1, in which  $\mathbf{q}$  and  $\mathbf{q}'$  are parallel. Now we are concerned only with three modes; the upper polariton, the lower polariton and the THz photon. Their in-plane wave vectors are fully determined by the argument above, so we can simplify the notation omitting the wave vectors for the quantities relative to these modes.

The spontaneous emission matrix element in Eq. (5) is not enough on its own to let us calculate the THz emission in the stimulated regime; instead we need the full many body matrix element describing a transition from a state with  $N_{UP}$  upper polaritons,  $N_{LP}$  lower polaritons and  $N_{THz}$  THz photons to a state in which an upper polariton has become a lower one, emitting a THz photon. Were intersubband excitations elementary bosons, the transition rate would be exactly equal to the spontaneous rate times the bosonic enhancement rate  $N_{UP}(N_{LP} + 1)(N_{THz} + 1)$ . However, intersubband excitations behave as composite bosons [19], implying that the bosonic enhancement factor is renormalized by the bosonicity factor  $B_{N_{UP}}^{N_{LP}} < 1$ , which depends on the populations of the initial state [3]. For normalized excitation densities  $\frac{N_{UP} + N_{LP}}{N} \ll 1$ , this coefficient can be well approximated by  $B_{N_{UP}}^{N_{LP}} \simeq 1 - \zeta_{LP} \frac{N_{LP}}{N} - \zeta_{UP} \frac{N_{UP}}{N}$ , where  $\zeta_{LP}$  and  $\zeta_{UP}$ , each of the order of one, depend on the Hopfield coefficients of the polariton modes. Notice that a state with polaritonic populations  $N_{UP}$  and  $N_{LP}$  corresponds to a linear superposition of states which has, at most,  $N_{UP} + N_{LP}$  electrons in the excited subband.

Denoting the linewidths of the different modes as  $\Gamma_{UP}$ ,  $\Gamma_{LP}$  and  $\Gamma_{THz}$ , and assuming, for simplicity, that the lower polariton has a Lorentzian lineshape, the spontaneous scattering rate  $\Xi_s$  for the considered interbranch dipole transition can be approximated via the Fermi golden rule as

$$\Xi_s = \frac{\omega_{THz}(\Delta z e y_{UP} y_{LP})^2}{2\hbar\epsilon_0\epsilon_r S L_{cav}} \int d\omega \frac{\Gamma_{LP}\delta(\omega_{UP} - \omega_{THz} - \omega)}{(\omega - \omega_{LP})^2 + (\frac{\Gamma_{LP}}{2})^2}, \quad (6)$$

where we have assumed, as is usually the case experimentally, that the width of the lower polariton mode is much larger than that of the THz photon mode ( $\Gamma_{LP} \gg \Gamma_{THz}$ ). For the resonant, stimulated process, this becomes

$$\Xi(N_{UP}, N_{LP}, N_{THz}) = \frac{2B_{N_{UP}}^{N_{LP}}\omega_{THz}(\Delta z e y_{UP} y_{LP})^2}{\hbar\epsilon_0\epsilon_r S L_{cav}\Gamma_{LP}} \quad (7)$$

$$\times [N_{UP}(N_{LP} + 1)(N_{THz} + 1) - (N_{UP} + 1)N_{LP}N_{THz}].$$

If we denote the pumping rate into the upper polariton mode as  $P$ , we can thus write the following rate equation for the populations in the three modes

$$\begin{aligned} \dot{N}_{UP} &= -\Gamma_{UP}N_{UP} - \Xi(N_{UP}, N_{LP}, N_{THz}) + P \\ \dot{N}_{LP} &= -\Gamma_{LP}N_{LP} + \Xi(N_{UP}, N_{LP}, N_{THz}) \\ \dot{N}_{THz} &= -\Gamma_{THz}N_{THz} + \Xi(N_{UP}, N_{LP}, N_{THz}). \end{aligned} \quad (8)$$

In the limit  $B_{N_{UP}}^{N_{LP}} \simeq 1$ , we can solve Eq. (8) for its steady state and compute the quantum efficiency as

$$\eta = \frac{x_{UP}^2 \Gamma_{THz} N_{THz}}{P} = \frac{x_{UP}^2 \max[1 - \frac{\Gamma_{UP}\Gamma_{THz}}{\Xi_s P}, 0]}{1 + \frac{\Gamma_{UP}}{\Gamma_{LP}}}, \quad (9)$$

where the Hopfield coefficient  $x_{UP}$  accounts for the fact that the pump beam couples only to the photon part of the upper polariton. From Eq. (9) it is possible to verify that, as we anticipated, extremely high quantum efficiencies can be achieved going toward higher pump powers. We can also write the condition for stimulated THz emission to be possible as  $\Xi(N_{UP}, 0, 0) > \Gamma_{THz}$ . From Eq. (7) the threshold density for stimulated emission, neglecting  $B_{N_{UP}}^0$ , is then

$$\frac{N_{UP}}{S} = \frac{\Gamma_{THz}}{\omega_{THz}} \frac{\hbar\epsilon_0\epsilon_r L_{cav}\Gamma_{LP}}{2(\Delta z e y_{UP} y_{LP})^2}. \quad (10)$$

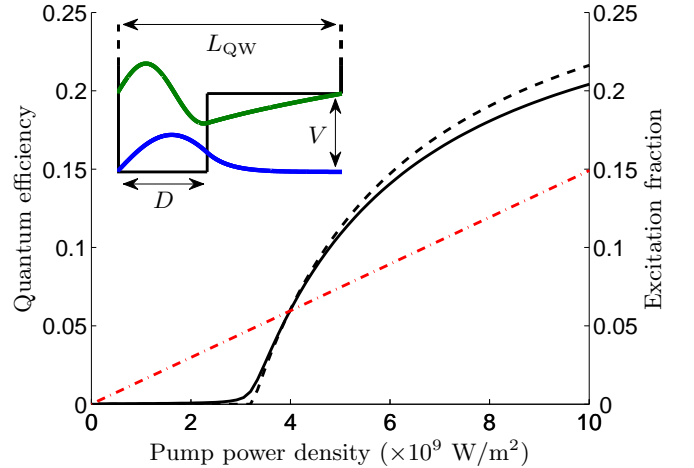


FIG. 2: Black solid line: quantum efficiency  $\eta$  as a function of the applied pump power density calculated solving numerically Eq. (8), including thus nonbosonicity effects. Black dashed line: same quantity obtained using Eq. (9). Red dash-dotted line: total excitation fraction  $\frac{N_{UP} + N_{LP}}{N}$ . Inset: wavefunctions for the first two conduction subbands for an asymmetric GaAs quantum well structure. Due to the quantum well asymmetry,  $\Delta z = \langle \psi_2 | z | \psi_2 \rangle - \langle \psi_1 | z | \psi_1 \rangle \neq 0$ . All the parameters are given in the text.

Using this formalism to predict quantitative conversion efficiencies requires us to consider a specific example structure. In general, a compromise is needed to get a large enough  $z_{12}$  to achieve the strong-coupling required to create a polariton frequency splitting in the THz range and a large enough  $\Delta z$  to have an interbranch transition dipole. As an example we consider the simple asymmetric stepped GaAs quantum well of Fig. 2 with infinite barriers. It is characterized by only three parameters, the overall width,  $L_{QW}$ , the height,  $V$ , and

the position,  $D$ , of the potential step. The wavefunctions shown in Fig. 2 correspond to  $L_{QW} = 25$  nm,  $D = 0.4L_{QW}$  and  $V = 138$  meV; this gives an ISBT energy  $\hbar\omega_{12} \simeq 100$  meV and  $\Delta z \simeq z_{12} \simeq 0.1L_{QW}$ . These values are not optimal, but similar ones are obtainable in a fairly large sector of the parameter space and we thus expect them to be easily achievable also in more realistic geometries. We model a structure composed of  $n_{QW} = 40$  such GaAs QWs each doped at an electron density  $N_{2DEG} = 10^{12}$  cm $^{-2}$ , that gives a resonant vacuum Rabi frequency  $\Omega(q_{res}) \simeq 0.1\omega_{12}$  [where  $q_{res}$  is the resonant wave vector such that  $\omega_{ph}(q_{res}) = \omega_{12}$ ]. Assuming  $y_{UP} \simeq 0.6$  and  $y_{LP} \simeq 0.9$  (the values of the process represented in Fig. 1), a quality factor for the THz mode  $\frac{\omega_{THz}}{\Gamma_{THz}} = 100$  [22] and polaritonic linewidths  $\Gamma_{UP} = \Gamma_{LP} = 4$  meV [20], Eq. (10) gives  $\frac{N_{UP}}{N} \simeq 0.05$ , that is to say that the onset of stimulated THz emission occurs when only  $\simeq 5\%$  of the electrons are in the excited subband. Such low excitation threshold density justify *a posteriori* the approximation of neglecting the nonbosonicity factor in Eq. (10).

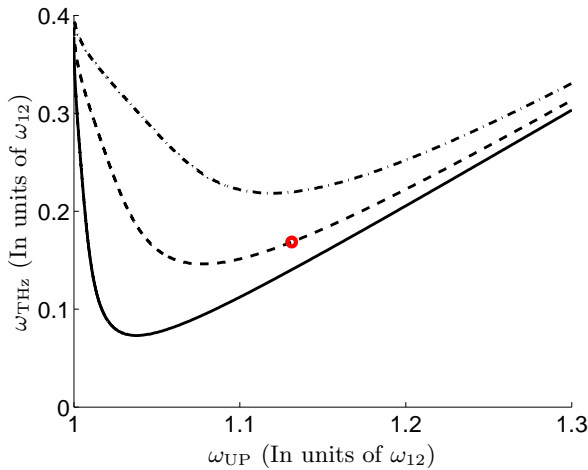


FIG. 3: Frequency of the emitted THz radiation  $\omega_{THz}$ , considering forward scattering, as a function of the pump frequency  $\omega_{UP}$ . The different lines correspond to  $\frac{\Omega}{\omega_{12}} = 0.05$  (solid line), 0.1 (dashed line) and 0.15 (dash-dotted line). The red circle marks the parameters considered for the numerical application in the text.

This offers the possibility of demonstrating a THz inversionless laser [23, 24]. In Fig. 2 we see the quantum efficiency as a function of the pump power obtained by numerically solving Eq. (8) (solid black line) and using Eq. (9), that is, neglecting nonbosonicity effects (black dashed line). In the same Figure we also plot the total excitation density  $\frac{N_{UP} + N_{LP}}{N}$  as a function of the pump power (red dash-dotted line). We see that, with experimentally achievable pump powers [25], a quantum conversion efficiency in excess of 20% is possible, still with the system being a long way from population inversion.

In Fig. 3 we explore the versatility of this system by studying the way the forward-scattered emitted THz photon frequency  $\omega_{THz}$  depends on the pump frequency  $\omega_{UP}$ , for different values of the light-matter coupling  $\Omega(q_{res})$ . At lower values of  $\Omega(q_{res})$  the mechanism gives a frequency down-conversion up to a factor 10, while staying in the strong coupling regime and maintaining large conversion efficiencies. Since  $\Omega(q_{res})$  can be modulated by electronically changing the electron gas density [15, 17], this offers a way of realizing widely tunable THz emitters.

In conclusion we have shown how, through the use of asymmetric QWs in intersubband polariton systems, it is possible to obtain stimulated THz emission characterized both by an extremely large quantum efficiency and a remarkable frequency tunability.

We would like to thank I. Carusotto, L. Nguyen-thê, C. Sirtori and Y. Todorov for useful discussions. C.C. is member of Institut Universitaire de France. We acknowledge support from the ANR project THINQE-PINQE.

- 
- [1] S. Haroche and J.-M. Raimond, *Exploring the quantum: atoms, cavities, photons*, (Oxford Press, 2006).
  - [2] B. Deveaud (Ed.), *The physics of semiconductor microcavities*, (Wiley-VCH, 2007).
  - [3] S. De Liberato and C. Ciuti, Phys. Rev. Lett. **102**, 136403 (2009).
  - [4] K. V. Kavokin *et al.*, Appl. Phys. Lett. **97**, 201111 (2010).
  - [5] I. G. Savenko, I. A. Shelykh and M. A. Kaliteevski, Phys. Rev. Lett. **107**, 027401 (2011).
  - [6] E. del Valle and A. Kavokin, Phys. Rev. B **83**, 193303 (2011).
  - [7] Faist *et al.*, Science **264**, 553 (1994).
  - [8] R. Koehler *et al.*, Nature **417**, 156-159 (2002).
  - [9] Y. Chassagneux *et al.*, Nature **457**, 174 (2009).
  - [10] S. De Liberato and C. Ciuti, Phys. Rev. B **79**, 075317 (2009).
  - [11] D. Dini *et al.*, Phys. Rev. Lett. **90**, 116401 (2003).
  - [12] C. Ciuti, G. Bastard and I. Carusotto, Phys. Rev. B **72**, 115303 (2005).
  - [13] A. A. Anappara *et al.*, Phys. Rev. B **79**, 201303 (2009).
  - [14] Y. Todorov *et al.*, Phys. Rev. Lett. **105**, 196402 (2010).
  - [15] A. A. Anappara *et al.*, App. Phys. Lett. **87**, 051105 (2005).
  - [16] A. A. Anappara *et al.*, Appl. Phys. Lett. **91**, 231118 (2007).
  - [17] G. Günter *et al.*, Nature **458**, 178 (2009).
  - [18] M. Geiser *et al.*, Phys. Rev. Lett. **108**, 106402 (2012).
  - [19] M. Combescot, O. Betbeder-Matibet and R. Combescot, Phys. Rev. B **75**, 174305 (2007).
  - [20] S. Luin *et al.*, Phys. Rev. B **64**, 041306 (2001).
  - [21] S. De Liberato and C. Ciuti, Phys. Rev. B **85**, 125302 (2012).
  - [22] A. Andronico *et al.*, Opt. Lett. **33**, 2416 (2016).
  - [23] M. D. Frogley *et al.*, Nature Materials, **5**, 175 (2006).
  - [24] J. Gambari *et al.*, Phys. Rev. B **82**, 121303 (2010).
  - [25] J. F. Dynes *et al.*, Phys. Rev. Lett. **94**, 157403 (2005).